JOHANNES GUTENBERG
UNIVERSITÄT MAINZ

Long range interactions in kinetic Monte-Carlo simulations

(Langreichweitige Wechselwirkungen in kinetischen Monte-Carlo Simulationen)

von

Timo Pulch

Bachelorarbeit in Physik
vorgelegt dem Fachbereich Physik, Mathematik und Informatik (FB 08)
der Johannes Gutenberg-Universität Mainz
am 15. Februar 2018

1. Gutachter: Prof. Dr. Kremer
2. Gutachter: Dr. Virnau

Ich versichere, dass ich die Arbeit selbstständig verfasst und keine anderen als die angegebenen Quellen und Hilfsmittel benutzt sowie Zitate kenntlich gemacht habe.

Mainz, den 15.02.2018

Timo Pulch
Institut für Physik
Staudingerweg 7
Johannes Gutenberg-Universität D-55099 Mainz
tpulch@students.uni-mainz.de

Contents

1. Zusammenfassung

In dieser Thesis wird gezeigt werden, dass die “Image Charge MMM2D” (ICMMM2D) eine geeignete Methode ist um langreichweitige Wechselwirkung in Kinetisches Monte Carlo Simulationen zu beschreiben, die im VOTCA Paket durchgeführt werden. Es wird sich zeigen, dass bekannte Methoden wie die Ewald-Summation nur bedingt für spezielle Geometrie geeignet sind. Des weitern wird sich zeigen, dass ICMMM2D Methode dielektrische Grenzflächen richtig handhabt und dazu genutzt werden kann die Paarwechselwirkungsmartix in Plattengeometrien zu berechnen, welche benötigt werden für die Berechnung der Raten im KMC Paket von VOTCA. Dies wird durch den Vergleich der Ergebnisse des ICMMM2D, der Direktsumme der Coulomb Wechselwirkung und eines klassischen, dielektrischem Kontinuumsmodels gezeigt werden.

2. Abstract

In this thesis will be shown that the Image Charge MMM2D (ICMMM2D) method is an appropriate approach to deal with long range interaction in Kinematic Monte-Carlo simulations that will be performed with the VOTCA-package. We will highlight that it is not possible to use well-known methods such as Ewald summation in each geometry. It will be shown that the ICMMM2D method treats dielectric boundaries correctly and is possible to calculate the pair interaction matrixes for slab geometries which are needed for the rate calculation in KMC package of VOTCA. This will be done by the comparison of the results of ICMMM2D with the result of a direct sum and a classical dielectric continuum model.

3. Introduction

The invention of organic light emitting diodes (OLEDs) facilitated the development of an active-matrix display (AMOLED). The key properties of organic semiconducting materials useful for this application are their cost-effectiveness, enhanced processibility, and tunability of electronic properties [3]. Nevertheless, there is still need for improvement and innovation, especially for stable blue OLEDs which currently prevent further applications, such as white light sources due to there short lifetime. The understanding of the elementary processes that are taking place in such devices is the foundation towards new materials and improved designs.
In Figure 3.1 a schematic of a phosphorescent OLED is shown. A typical OLED consists of a layer of organic material in between two electrodes, an anode and a cathode, deposited on a substrate. By conjugation of molecules, electrical conductivity is reached through the overlapping $\pi-$orbitals and delocalization of respective $\pi-$electrons in the organic material. Analogous to valence and conducting the band in ordinary semiconductor one defines the highest occupied and lowest unoccupied molecular orbitals (HOMO and LUMO) of organic semiconductors. Examples of materials are shown in figure 3.1. By injection electrons in the LUMO of the organic material next to the cathode and withdrawing electrons from the HOMO at the anode (injecting holes) an electric current starts to flow. These holes and electrons are driven together by electric forces and form excitons, a bound state of an electron and a hole . Radiation is a result of the decay of these excited states. The current-voltage-luminescence characteristics are then related to an interplay between electron, hole, and exciton mobilities, their relative energy offsets, as well as energetic disorder and recombination rates.

Computer simulations are used to study the morphological order and molecular structure regarding device efficiency. This is a computationally demanding task which is impossible to perform on a quantum mechanic level only, especially for layers of a few hundred nanometers. One has to employ classical force-fields, first principle methods to evaluate charge/exciton transfer rates, and a develop stochastic models based on the master equation, as illustrated in Figure 3.2. This theoretical approach often relies on experimental input, e.g. experimentally measured mobility values. Further weaknesses are that these models often rely on approximations and parametrizations in quasi-static conditions, but used to make predictions in non-equilibrium systems. A model which does not require explicit simulation of atomistic morphologies and quantum-chemical evaluated rates is constructed by matching mesoscopic system properties, like distributions of molecular positions and orientation, electronic couplings, and site energies. This so-called off-lattice model is used to describe large systems [11]. Quantities like potential energy surface, reorganization energy, ionization potential, and

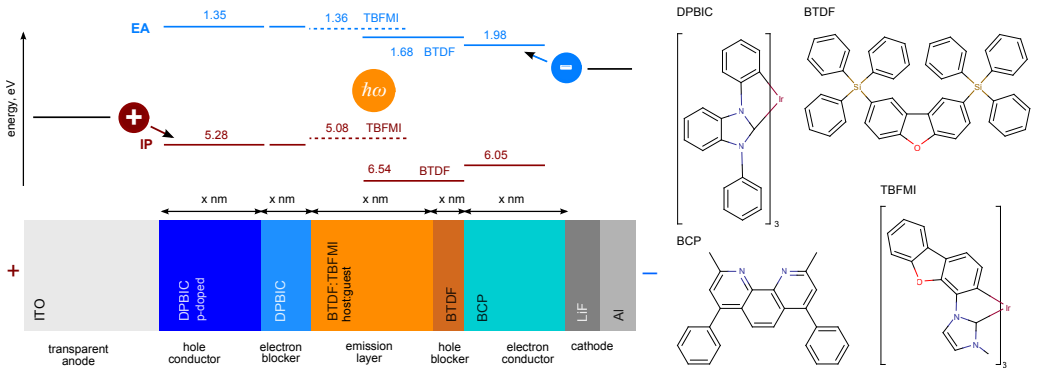

Figure 3.1.: Multilayered structure of an OLED with corresponding energy levels and chemical structures. Electrons/holes move upward/downward in energy due to an applied voltage. Higher electron/hole energy levels correspond to smaller electron affinities/ionization potentials. In this OLED, DPBIC (Tris[(3-phenyl-1H-benzimidazol-1-yl-2(3H)-ylidene)-1,2-phenylene]Ir) is used in the hole-conducting layer; TBFMI (Tris[(1,2-dibenzofurane- 4-ylene)(3-methyl-1/1-imidazole-1-yl-2(3/1)-ylidene)]Ir(III)) is the emitter (guest); BTDF (2,8-bis(triphenylsilyl)dibenzofurane) is the host material and 2,9-dimethyl-4,7-diphenyl-1,10-phenanthroline (bathocuproine, BCP) is the electron conductor. Adapted with permission from Kordt et al., 25, Advanced Functional Materials 1955-1971 (2015). Copyright (2015) Wiley-VCH Verlag Gmbh [11].

electron affinity, as well as distributed multipoles and polarization, are calculated via first principle methods for each molecule type. These are used to evaluate the classical force-fields in a further step to simulate amorphous morphologies. In chapter 2, a perturbative approach is briefly discussed which is used to evaluate the electrostatic and induction interactions of localized charge carriers with the environment via polarized force-fields.

By taking all these quantities into account, it is possible to evaluate rates for charge/exciton transport in a system of around 10^4 molecules by combining first principle methods and classical force-fields [11]. In organic semiconductors, Charge/exciton transport happens through so-called hopping events, where a charge/exciton hops form on site i to a different site j. For this, we need to know the site energy of interacting sites particularly the energy difference between the sites. Because the systems tend to favour a state of lower energy the energy difference is relevant. An important ingredient of the charge transfer rate is the free energy difference between the final and initial states of the system. A part of this energy is the Coulomb interaction of charges. This interaction is long range and therefore is computationally demanding and often needs special treatment in the periodic boundary conditions that are typically applied in molecular systems.

By hopping from site i to j, the configuration of the system has changed more precisely the state of the system has changed. By precomputing the rates of a certain state, we can formulate the master equation, a differential equation of first order, which describes the time-dependent probability of the system to transit from one state to another one, i.e. the time evolution of a system. By solving the master equation

the charge carrier mobility and occupation probability of the considered systems are determined. Concerning the system of interest, the only sufficient way to solve the master equation is introduced in chapter 3 namely the Kinematic Monte Carlo (KMC) method, due to a large amount of states which needed to be taken into account. By solving the system via KMC, we reset the memory of the system in each step, what means each calculation of a further configuration just require the present configuration as a starting point. This resetting requires the evaluation of the rates in each step over and over again.
Unfortunately, this is a computation demanding task, especially for a large system. The extended computational cost is mainly due to the influence of Coulomb interaction on the rates. A variety of methods has been developed to treat with Coulomb interactions in such systems. However, difference geometries or neutrally charged systems that we are considering need special treatment. Therefore, we are going to introduce efficient schemes that are used to calculate the Coulomb interaction in such systems to solve the master equation via KMC. Efficient schemes for treatment of Coulomb interactions and their integration into the master equation is the topic of this thesis.

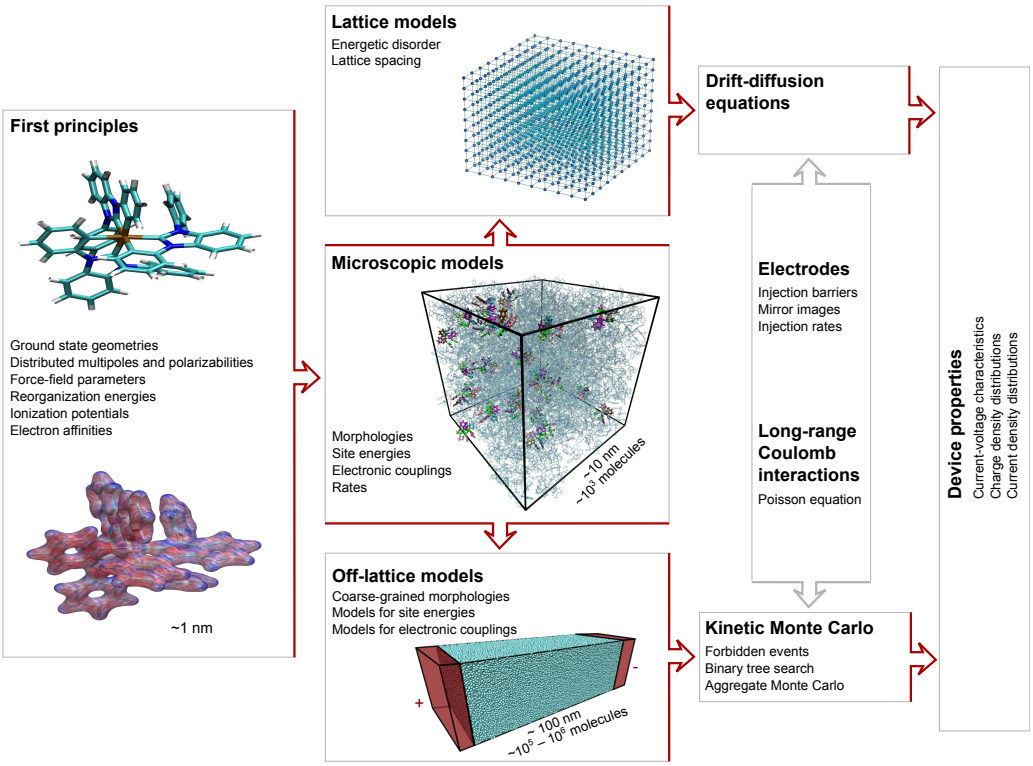

Figure 3.2.: Possible workflows of parameter-free OLED simulations: polarizable force-fields and electronic properties of isolated molecules obtained from first principles are used to generate amorphous morphologies and evaluate charge transfer rates in small systems (microscopic models). Coarse-grained models are parametrized either by matching macroscopic observables, e.g., charge mobility, of the microscopic and coarse-grained (lattice) models. The resulting analytical expressions for mobility are then used to solve drift-diffusion equations for the entire device, after incorporating long range electrostatic effects and electrodes. Alternatively, off-lattice models can be developed by matching distributions and correlations of site energies, electronic couplings, and positions of molecules. The master equations for this model can be solved using the kinetic Monte Carlo algorithm, yielding macroscopic characteristics of a device. Adapted with permission from Kordt et al., 25, Advanced Functional Materials 1955-1971 (2015). Copyright (2015) Wiley-VCH Verlag Gmbh [11].

4. Intermolecular Interactions

We are interested in finding a appropriate formalism to calculate the energy difference for a charge that is hopping from site i to j. In soft matter intermolecular forces are electrostatics, dispersion and induction. In the perturbative description of these interactions, the electrostatic interactions is mediated between classical charge distributions. Through distortion of electron clouds in electric fields, dipoles are created within molecules. The interaction of these dipoles with the surrounding molecules is called induction. The effect that manifest through the fluctuations of the electron densities and the correlation of these in two different molecules is called dispersion. An accurate way to do describe the electrostatic interaction in molecular systems is the Thole model [14]. It relies on introducing a force field via multipole expansion and taking into account induction. In the following we will mostly look at the effect of charge-charge interaction and add the effect of the electric neutral environment through a precalculated density of states.

4.1. Pertrubation Theory

Because intermolecular forces are fairly weak, it is common to describe them using perturbation theory. We will see that starting from a quantum mechanical description we can find the classical expressions by averaging over different orders of perturbation. Furthermore, multipoles and distributed multipoles will be introduced because we are mainly interest to calculate dipole-dipole interactions. To do this, we need to assume that there wave functions do not overlap due to a large distance between them. The unperturbed Hamiltonian of a combined system H' regarding the electrostatic interaction between molecule A and molecule B is:

$$H' = \int \sum_{a\in A}\sum_{b\in B} \frac{e_a\delta(\mathbf{r}-\mathbf{a})e_b\delta(\mathbf{r'}-\mathbf{b})}{4\pi\epsilon_0|\mathbf{r}-\mathbf{r'}|}d^3\mathbf{r}d^3\mathbf{r'} = \int \frac{\tilde{\rho}^A(\mathbf{r})\tilde{\rho}^B(\mathbf{r'})}{4\pi\epsilon_0|\mathbf{r}-\mathbf{r'}|}d^3\mathbf{r}d^3\mathbf{r'} \tag{4.1}$$

where we use the charge density operator of molecule X: $\tilde{\rho}^X(\mathbf{r}) = \sum_{x\in X} e_x\delta(\mathbf{r}-\mathbf{x})$. Now one can write the unperturbed states as simple product functions $\Psi_m^A\Psi_n^B$, which we shorten to $|mn>$ and are eigenfunctions of H^0. This is our starting point to use Rayleigh-Schrödinger perturbation theory for closed-shell molecules to derive the second order ground state energy, labeled $m = n = 0$. By averaging over the Hamiltonian we are going form a quantum mechanical Coulomb interaction to classical interpretations as electrostatic interaction, induction and dispersion energy.

$$< 00|H_0^0|00 >= W_{00} + W'_{00} + W''_{00} + ... \tag{4.2}$$

where

$$W_{00}^{0} = W_{0}^{A} + W_{0}^{B}, \tag{4.3}$$

$$W_{00}^{\prime} =< 00|H^{\prime}|00 >, \tag{4.4}$$

$$W_{00}^{\prime\prime} = -\sum_{nm} \frac{< 00|H^{\prime}|mn >< mn|H^{\prime}|00 >}{W_{m}^{0}n - W_{00}^{0}}. \tag{4.5}$$

This is the perturbative approximation to the interaction energy, where the first-order energy in eq. 4.4 is the expectation value of the electrostatic interaction of the ground state $|00>$. The second-order terms can be identified as induction energy and dispersion energy in the manner:

$$W^{\prime\prime} = U_{ind}^{A} + U_{ind}^{B} + U_{disp} \tag{4.6}$$

where

$$U_{ind}^{A} = -\sum_{m\neq 0} \frac{< 00|H^{\prime}|m0 >< m0|H^{\prime}|00 >}{W_{m}^{A} - W_{0}^{A}} \tag{4.7}$$

$$U_{ind}^{B} = -\sum_{m\neq 0} \frac{< 00|H^{\prime}|0n >< 0n|H^{\prime}|00 >}{W_{n}^{B} - W_{0}^{B}} \tag{4.8}$$

$$U_{dis} = -\sum_{m\neq 0} \frac{< 00|H^{\prime}|mn >< mn|H^{\prime}|00 >}{W_{M}^{A} + W_{n}^{B} - W_{0}^{B} - W_{0}^{A}} \tag{4.9}$$

A common way to calculate the electrostatic, induction and dispersion energy is to develop it into multipoles, but it may be mentioned that for short distances between molecules the sum in 4.6 does not converge and different techniques much are used. For the dispersion energy, the calculation is even harder, due to the factorization of the denominator is unlikely to the matrix elements referring to A and B not possible. There are two used ways to handle the problem one is the average-energy approximation and the second is based on the work in the field of quantum electrodynamics by Casimir and Polder (1948). For further details see [12].

4.2. Multipole Expansion

In terms of classical electrostatics the simplest multiple is the total charge $q = \sum_i e_i$, where e_i is the charge of particle i. If the system is placed in an electric potential field $V(\mathbf{r})$, the energy becomes

$$U_{es} = \sum_{i} e_i V(i), \tag{4.10}$$

where we are using the vector $\mathbf{i}$ to describe the position of particle i. In the case we assume an uniform electric field with the constant at the origin V_0, the arbitrary magnitude F and directions x, y, z it fallow

$$U_{es} = qV_0 - \sum_{k}\sum_{i}^{3} e_i a_k F_k = qV_0 - \vec{\mu}\cdot\mathbf{F}. \tag{4.11}$$

The quantity $\vec{\mu}$ is called dipole moment. In case of two positive and two negative charges one finds the quadrupole moment

$$\Omega_{kj} = \sum_i e_i(\frac{3}{2}i_k i_j - \frac{1}{2}i^2\delta_{kj}) \tag{4.12}$$

where i and k are out of (x, y, z). In the same manner one can expand these multipoles to any rank:

$$\zeta^{(n)}_{jk...z} = \frac{(-1)^n}{n!}\sum_i e_i a^{(2n+1)}\frac{\delta}{\delta i_z}...\frac{\delta}{\delta i_k}\frac{\delta}{\delta i_j}(\frac{1}{i}). \tag{4.13}$$

Going back to a quantum mechanical description the multipole expansion in terms of the Hamiltonian has the form :

$$H' = q^B V^A + \tilde{\mu}^B_\alpha V^A_\alpha + \frac{1}{3}\tilde{\Omega}^B_{\alpha\beta}V^A_{\alpha\beta} + ... \tag{4.14}$$

$$= Tq^A q^B + T_\alpha(q^A\tilde{\mu}^B_\alpha - \tilde{\mu}^A_\alpha q^B) + T_{\alpha\beta}(\frac{1}{3}q^A\tilde{\Omega}^B_{\alpha\beta} - \tilde{\mu^A_\alpha}\tilde{\mu}^B_\beta + \frac{1}{3}\tilde{\Omega}^A_{\alpha\beta}q^B) + ...,$$

where $T^n_{\alpha\beta...\nu} = \frac{1}{4\pi\epsilon_0}\nabla_\alpha\nabla_\beta...\nabla\frac{1}{\mathbf{R}}$ is the quantum analogous to 4.13 and $V^A(\mathbf{r}) = \int\frac{\tilde{\rho^A}(\mathbf{r})}{4\pi\epsilon_0|\mathbf{r}-\mathbf{r'}|}d^3\mathbf{r'}$ is the potential of molecule A relative to the center of mass A.

By averaging over this expression one find classical the electrostatic, induction and dispersion energy again, but now in terms of multipoles. At this point the transformation into spherical coordinates and the use of spherical harmonics **R** and **I** is convenient,

$$\frac{1}{|\mathbf{R}+\mathbf{b}-\mathbf{a}|} = \sum_{l=0}^{\infty}\sum_{m=-l}^{l}(-1)^m R_{l,-m}(\mathbf{a}-\mathbf{b})\mathbf{I}_{lm}(\mathbf{R}). \tag{4.15}$$

,where **a,b** are the vectors relative to the center of mass of the molecules A and B.

4.3. Distributed multipoles

The multipoles expansion series with the multipoles positioned in one center of mass of the moleculare are not accurate. To improve the accuracy, we can divide the molecule into regions, each described by its own multiple moments. This method is known as distributed multipole expansion. Such a region consisted of an atom or a group of atoms. The interaction between two molecules A and B then takes the form

$$H' = \sum_{a\in A}\sum_{b\in B}[T^{ab}q^A q^b + T^{ab}_\alpha(q^a\tilde{\mu}^b_\alpha - \tilde{\mu}^a_\alpha q^b] \tag{4.16}$$
$$+ T^{ab}_{\alpha\beta}(\frac{1}{3}q^A\tilde{\Omega}^b_{\alpha\beta} - \tilde{\mu}^a_\alpha\tilde{\mu}^b_\beta + \frac{1}{3}\tilde{\Omega}^a_{\alpha\beta}a^b + ...].$$

The sum runs over the sites a of molecule A and sites b of molecule B and $q^a, \tilde{\mu}^a_\alpha$ are the operators for the charge, dipole of site a and so on [12]. From here we can exactly apply the perturbation theory as before.

5. Kinetic Monte Carlo

5.1. Master equation

In the previous chapter, we have looked at an appropriate approach to deal with the electrostatic interaction of molecular system. Now we would like to have a look at the dynamics of charges because they change the state of a system. In organic semiconductor, charge transport is a series of so-called hopping events between adjusted sites. The hopping probability is proportional to a transition rate between different states. Due to a large number of molecules and atoms, there is no way to provide a quantum mechanical solution.
A stochastic model based on a master equation is a viable approach to proceed further. The systems of interest can be modelled as being in a probabilistic combination of states at any given time, and the corresponding switching between that states can be determined by a transition rate matrix. States are constituted of a combination of electrons which are sitting on occupied molecular sites. The time evolution of such systems is being described by a so-called master equation, or are a set of differential equations over time of the probabilities P_α that the system occupies each of different states α and has the following form:

$$\frac{d}{dt}P_\alpha = \sum_\beta [W_{\alpha\beta}P_\alpha(t) - W_{\beta\alpha}P_\beta(t)] \tag{5.1}$$

where P_α is the probability for the system to be in a certain state α, $W_{\alpha\beta}$ is the transition rate form state β to α. In a physical system, which is in an equilibrium state the *detailed balance* principle is fulfilled, and one speaks of a reversible Markov chain [10]

$$W_{\alpha\beta}P_\alpha(t) = W_{\beta\alpha}P_\beta(t). \tag{5.2}$$

In the case of amorphous semiconductors, each site corresponds to a molecule.
In practice, one has to solve a system of coupled, linear, first order, ordinary differential equations (ODE) to evaluate the molecule position and the transfer rates ω_{ij}. Typically, the center of mass of a molecule is chosen as the position of the hopping site. Given the rate $\omega_{\alpha\beta}$ the occupation probabilities P_α can be determined [10].
For large systems an analytic solution of the master equation is impossible. Therefore one relies on approximations such as Mean Fields or the Kinetic Monte Carlo method.

5.2. Mean-field solution

In a system with many charge carriers, a given state α of a system is definded through sites occupied by charges. The number of rates grows exponentially with the number of charges, even advanced ODE solvers become impractical unless further approximations are made. One of the most used is the mean-field approximation. When the master equation is rewritten in terms of site-occupation probability p_i all correlations between the occupation probabilities of different sites are neglected [4]. The rewritten master equation, electron transform rates and occupation probabilities has the form:

$$\frac{d}{dt}p_i(t) = \sum_j [\omega_{ij} p_i(t)(1 - p_j(t)) - \omega_{ji} p_j(t)(1 - p_i(t))]. \tag{5.3}$$

with a constraint on the total probability being the number of charges carries:

$$n = \sum_i p_i. \tag{5.4}$$

It is possible to solve these nonlinear, differential equations with ODE algorithms, but these algorithms are much more complicated. The Kinetic Monte Carlo method is often more efficient and does not neglect correlation between the different sites [**?**].

5.3. Solving the Master equation via Variable Step Size Method

5.3.1. The integral from of the master equation

The fundamental concept of kinetic Monte Carlo (KMC) are Markov chains. Markov chains are statistic models, which allow the prediction of future without knowing the history [6]. In case of KMC just the present configuration is needed to be known.
To solve the master equation with Kinetic Monte Carlo methods casting the master equation into an integral form is a frequently used approach. A matrix $\mathbf{W}$ is assumed with zero diagonal ($W_{\alpha\alpha} = 0$) and a diagonal matrix $\mathbf{R}$

$$\mathbf{R}_{\alpha\beta} = \left\{ \begin{array}{l} 0, \text{ if } \alpha \neq \beta \\ \sum_\gamma W_{\gamma\beta}, \text{ if } \alpha = \beta. \end{array} \right\} \tag{5.5}$$

is defined .The probabilities of the configuration P_α are stored in a vector $\mathbf{P}$, we can rewrite master equation as a time-dependent Schrödinger-equation with an imaginary time and Hamiltonian **R - W**,

$$\frac{d\mathbf{P}}{dt} = \textbf{-(R -W)P}. \tag{5.6}$$

By assuming that $\mathbf{R}$ and $\mathbf{W}$ are time-independent and introducing a new matrix $\mathbf{Q}$,

$$\mathbf{Q}(t) = e^{(-\mathbf{R}t)}, \tag{5.7}$$

one can rewrite the solution of the master equation in the integral form [9],

$$\mathbf{P}(t) = \mathbf{Q}(t)\mathbf{P}(0) + \int_0^t dt' \mathbf{Q}(t-t').\mathbf{W}\mathbf{P}(t') \tag{5.8}$$

Due to the fact that 5.8 is implicit in $\mathbf{P}$, one can substitute $\mathbf{P}(t')$ over and over again and get

$$\begin{aligned}\mathbf{P}(t) = [\mathbf{Q}(t) + \int_0^t dt' \mathbf{Q}(t-t')\mathbf{W}\mathbf{Q}(t') \\ + \int_0^t dt' \int_0^{t'} dt'' \mathbf{Q}(t'-t'')\mathbf{W}\mathbf{Q}(t'-t'')\mathbf{W}\mathbf{Q}(t'') + ...]\mathbf{P}(0)\end{aligned} \tag{5.9}$$

The integral from has a useful interpretation, suppose that the system at $t = 0$ is in the configuration α with probability $P_\alpha(0)$. The first term describes that the system is still in state α up to time t, i.e. no reaction has taken place, with probability $Q_{\alpha\alpha}(t)P_\alpha(0) = e^{(-\mathbf{R}_{\alpha\alpha t})}P_\alpha(0)$. The matrix $\mathbf{W}$ specifies the change in probability when a reaction happens. The second term represents the contribution to the probabilities when a reaction took place at t' and no reaction took place between times 0 and t'. The terms of higher order are subsequent continued for further events so that we are able to describe the time evolution based on our starting configuration $P(0)$.

5.3.2. The Variable Step Size method

A KMC algorithm can be directly derived from the found integral formalism. From a given state a range of configurations with the correct probability is generated by these algorithms. The idea is to set-up a given starting configuration, specify the transition rates between all states, let a jump event occur, update the system and time while resetting the memory of the system until the stop condition is fulfilled.

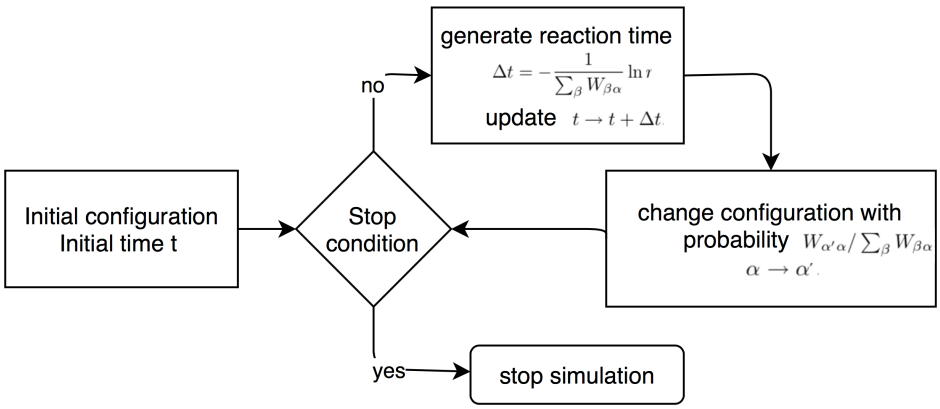

Figure 5.1.: Visualization of Variable Step Size Method

To do this in a mathematical accurate fashion one has to start from an initial time $t = 0$ and an initial configuration α. The probability that the system stays in configuration α is given by

$$\mathbf{Q}_{\alpha\alpha} P_\alpha(0) = e^{[-\mathbf{R}_{\alpha\alpha} t]} P_\alpha(0) \text{ resp. } \mathbf{Q}_{\alpha\alpha} = e^{[-\mathbf{R}_{\alpha\alpha} t]} \tag{5.10}$$

Obviously, the probability distribution that a reaction had taken place at time t is given by $1 - \mathbf{Q}_{\alpha\alpha}$. According to the probability distribution, we can find a time t' when the first reaction takes place by solving

$$e^{[-\mathbf{R}_{\alpha\alpha} t']} = r_1 \tag{5.11}$$

where r_1 is a uniform deviate on the unit interval [9]. Typically the time interval Δt is given by

$$\Delta t = \frac{1}{\sum_\beta W_{\beta\alpha}} \ln\, r \tag{5.12}$$

We know form eq. 5.9 that the transition possibility $W_{\beta\alpha}$ is given by all possible reactions that are transforming configuration α to β when a reactions happen at time t'. This on the other hand means that the probability of the system to be in state β at time $t' + dt$ is $W_{\beta\alpha} dt$. We can generate a new configuration α' at time t' by picking it out of β with probability $W_{\alpha'\alpha} / \sum_\beta W_{\beta\alpha}$. This process corresponds to resetting the memory of the system because we are in the same situation as when the simulation started. We continue these steps with t'', r_2 and configuration α'' until the end conditon is fulfilled.

5.3.3. Enabled and disabled events

Unfortunately, the VSSM algorithm scales with the system size exponentially because we need to sum over all possible configurations even the ones that will not physically be relevant. By introducing enabled events which leads to physically realised states, the performance can be improved. Enabled events are in terms of organic semiconductors hopping events between adjusted sites with hopping probability $W_{\beta\alpha} \neq 0$. A linearly scaling is achieved by storing these enabled events in one event list.
A further modification can be made to improve the efficiency, by considering that it is not necessary to evaluate all enabled events for each reaction, only the ones which are affected by a reaction will be sufficient. In the context of charge transport, an electron on a site, i, can hop to a neighbouring site, j. In doing so, all events associated with i are disabled, and all events associated with j are enabled.
These improvements lead to an algorithm which does not rely on calculating all enabled events in each iteration step over and over again. Instead, it just updates the list of enabled events, from previously disabled events after a reaction takes place. Concerning the charge transport problem, the interpretation will be that after a hop took place from α to β the hopping partners of α and β will be updated.
Considering this activation and deactivation procedure, we can implement an algorithm which treats charge transfer efficiently. Charge movement is assumed to occur

between sites $i = 1.....N$. The transport rate $W_{\beta\alpha}$ is interpreted as *hopping rate* ω_{ij} between different molecule sites i and j.
By assuming a system of N sites with $n < N$ charge carriers of one type, either electrons or holes, only the sites i which are occupied matter. For these sites escape rates to neighbours m can be defined in the way:

$$\omega = \sum_{j}^{m} \omega_{ij}. \tag{5.13}$$

In analogy to $W_{\alpha'\alpha}/\sum_\beta W_{\beta\alpha}$ a definition of the hopping probability form site i to j is given by $\omega_i/\sum_{k_{occupied}} \omega_k$ and the destination of a hop is chosen randomly by ω_{ij}/ω_i [11]. The scheme of VSSM method for multiple charge carrier will be:

STEP 1: Initialize a system of molecules with known escape rates.

STEP 2 : Inject charge carriers randomly.

STEP 3: Select an occupied site i which is proportional to $\omega = \sum_j^m \omega_{ij}$ by randomly drawing a number out of a uniform distribution.

STEP 4: Select a site j where the charge carrier is hopping to with the probability that is proportional to the hopping rate ω_{ij}.

STEP 5: Accept the hop if the site j is unoccupied or do not jump if the site j is occupied.

STEP 6: Update the time by drawing a second uniformly distributed random number τ. $t = t + \Delta t$, where $\Delta t = -(\sum_\beta W_{\beta\alpha})^{-1} ln\tau$. Go back to **STEP 3** if the stop condition is not fulfilled.

Nevertheless, there is a relevant part that we did not discuss the neighbour list. Since the systems of interest are treating with charge carriers, there will be Coulomb interaction we have not considered so far. The characteristic long-range interaction through the $1/r$ potential will affect carriers far away from the supposed hop and thereby lead to a large cut-off. Even if we assume forbidden events by prohibiting an occupied site to be occupied by a second charge carrier due to strong repulsive Coulomb force, there are still a large number of sites to be considered in the neighbour list, as well as escape rates needed to be updated in each iteration step. In the following sections, different ways to treat this problem efficiently will be described.

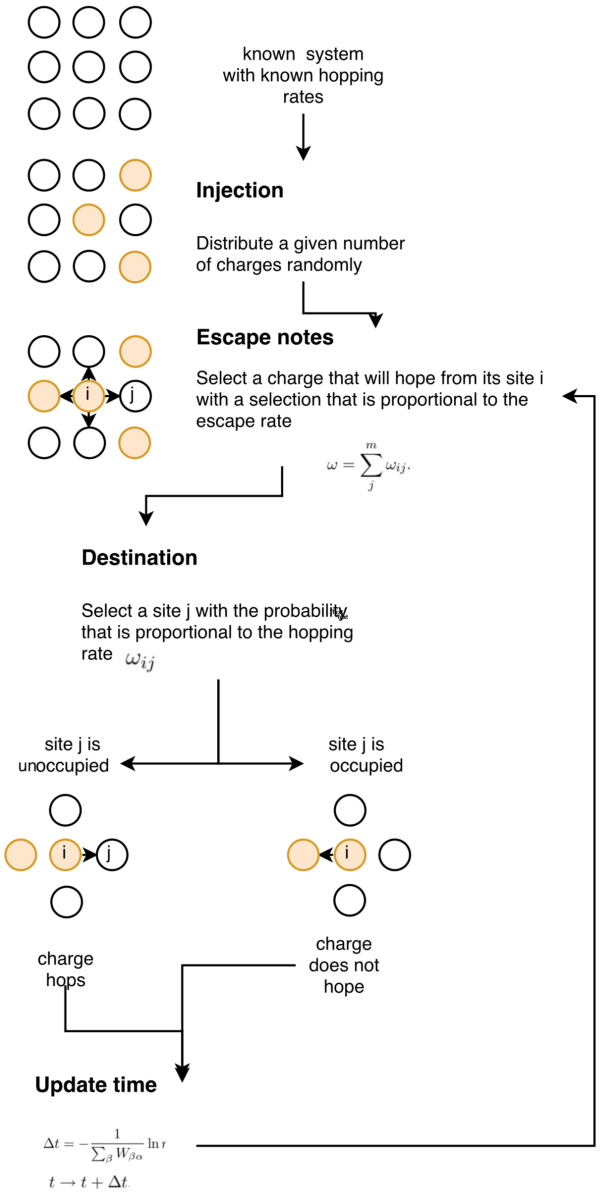

Figure 5.2.: Schematic visualization of two-level Monte Carlo method with multiple charge sites

6. Electrostatics

To determine the Coulomb interaction and finally the rates it is necessary to solve the Poisson equation for particular boundary conditions. This amounts to finding the electric potential ϕ for a given charge distribution ρ. Apparently, the solution for the Poisson equation takes different forms for different geometries. The general form of the Poisson's equation is:

$$-\nabla\Phi(\mathbf{r}) = 4\pi\rho(\mathbf{r}) \tag{6.1}$$

In this equation $\Phi(\mathbf{r})$ is the electrostatic potential, at point $\mathbf{r}$. For N point charges the charge distribution and the electrostatic potential has the following form:

$$\rho_P(\mathbf{r}) = \sum_{i=1}^{N} = q_i\delta(\mathbf{r} - \mathbf{r}_i) \tag{6.2}$$

$$\Phi(\mathbf{r}) = \sum_{i=1}^{N} \frac{q}{4\pi|\mathbf{r} - \mathbf{r}_i|}. \tag{6.3}$$

This sum takes into account periodic boundary conditions, what makes it difficult to calculate. By using the Fourier sum with the corresponding Fourier coefficients,

$$f(\mathbf{r}) = 1/V \sum_{k=-\infty}^{\infty} \tilde{f}(k)e^{i\mathbf{k}r} \ , \ \tilde{f}(\mathbf{k}) = \int d\mathbf{r} f(\mathbf{r})e^{-i\mathbf{k}r}, \tag{6.4}$$

where $k = \frac{2\pi}{L}$ is the reciprocal vector, V the box size, one will find a much simpler form for the Poisson's equation:

$$k^2\Phi(k) = 4\pi\rho(k). \tag{6.5}$$

There are many possible ways to solve the Poisson equation in the order of $O(N^2)$ or Cholesky solvers of order $O(S)$, but we are interested in those which are able to solve it fast for big systems. Therefore Fast Fourier Transformation (FFT) is a decent choice with a computational time of order $O(Nlog(N))$. For the FFT we consider a discrete Fourier transform (DFT) of a vector $(x_0, ..., x_{2n-1})$ of dimension $2n$ is given by:

$$f_m = \sum_{k=0}^{2n-1} x_k \cdot e^{-\frac{2\pi i}{2n}mk} \ m = 0, ..., 2n-1. \tag{6.6}$$

Where we differentiate indices with even numbers :

$$x'_k = x_{2k} \ k = 0, ..., n-1 \tag{6.7}$$

and uneven numbers:

$$x''_k = x_{2k+1} \; k = 0, ..., n-1. \tag{6.8}$$

The according $n-$dimensional DFT are f'_k and f''_k. This leads to:

$$\begin{aligned} f_m &= \sum_{k=0}^{n-1} x_{2k} e^{(-\frac{2\pi i}{2n} m(2k))} + \sum_{k=0}^{n-1} x_{2k+1} e^{(-\frac{2\pi i}{2n} m(2k+1))} \\ &= \sum_{k=0}^{n-1} x'_k e^{(-\frac{2\pi i}{2n} mk)} + e^{(-\frac{\pi i}{n} m)} \sum_{k=0}^{n-1} x''_k e^{(-\frac{2\pi i}{2n} mk)} \\ &= \left\{ \begin{array}{l} f'_m + e^{-\frac{\pi i}{n} m} \, , \; if \; m < n \\ f_{m-n} - e^{-\frac{\pi i}{n}(m-n)} \, , \; if \; m \geq n \end{array} \right\}. \end{aligned} \tag{6.9}$$

By calculating f'_m and f''_m $(m = 0, ..., n-1)$ f_m as well as f_{m+n} are determined in half the steps [8]. Considering small molecular system, FFT is not the best choice. The small system size leads to a large amount of Fourier modes which needed to be calculated and so we lose the advantages of the method.

6.0.1. Ewald summation

A well-known technique to evaluate the Coulomb interaction in periodic boundary conditions is the Ewald summation. The idea of Ewald summation is to calculate the Coulomb interaction of charge carriers efficiently by splitting the interaction in a short- and long-range sums. The short-range sum is calculated in real space and the long-range part is calculated in reciprocal space by using fast fourier transformation. The electrostatic potential in a periodic system has the the form:

$$\Phi(r_i) = \sum_{j,\mathbf{n}} \frac{q_j}{|\mathbf{r}_{ij} + \mathbf{n}L|}, \tag{6.10}$$

where we sum over all charge carriers j and over all periodic images $\mathbf{n}$. A further assumption will be to say that the delta function of point charges can be represented by a superposition of Gaussian functions which are smoothly varied to each other. These functions are called screened charge and screen background and have the shape.

$$\rho_{Gauß}(r) = -q_i(\alpha/\pi)^{3/2} e^{(-\alpha r^2)}. \tag{6.11}$$

Starting form these assumptions we can write the charge distribution as periodic sums of Gausssians:

$$\rho(r) = \sum_{j=1}^{N} \sum_{\mathbf{n}} q_j (\alpha/\pi)^{3/2} e^{-\alpha|\mathbf{r}-(\mathbf{r}_j+\mathbf{n}L)^2|}. \tag{6.12}$$

Fourier transforming the charge density yields

$$\rho(\mathbf{k}) = \sum_{j=1}^{N} q_j e^{-i\mathbf{k}\cdot(\mathbf{r}-\mathbf{r}_j)} e^{(-k^2/4\alpha)} \tag{6.13}$$

and can be inserted in the Poisson's equation

$$k^2\Phi(k) = 4\pi \sum_{j=1}^{N} q_j e^{(-i\mathbf{k}\cdot(\mathbf{r}-\mathbf{r}_j))} e^{(-k^2/4\alpha)} \tag{6.14}$$

This expression can be back transformed to real space and finally inserted into the electrostatic potential:

$$U = \frac{1}{2}\sum_i \rho(r_i) = \frac{1}{2V}\sum_{\mathbf{k}\neq 0} \frac{4\pi}{k^2} |\rho(\mathbf{k})|^2 e^{(-k^2/4\alpha)}. \tag{6.15}$$

At this point we twice counted the interaction between a continuous Gaussian charge cloud of charges q_i and point charges q_i located at the center of the Gaussian, this can be done by an correction of potential energy at the origin of a Gaussian charge cloud:

$$\rho_{Gauß}(r) = q_i(\alpha/\pi)^{3/2} e^{(-\alpha r^2)}. \tag{6.16}$$

Using spherical symmetry and the Poisson's equation the expression:

$$-\frac{1}{r}\frac{\partial^2}{\partial r^2} r\Phi_{Gauß}(r) = 4\pi\rho_{Gauß}(r) \tag{6.17}$$

double partial integration yields to:

$$\Phi_{Gauß}(r) = \frac{q_i}{r} erf(\sqrt{\alpha}r) \tag{6.18}$$

The limit $r > 0$ gives us the correction, or the self-interaction term:

$$U_{self} = (\alpha/\pi)^{\frac{1}{2}} \sum_{i=1}^{N} q_i^2 \tag{6.19}$$

We derive all equations to write the short-range electrostatic potential $\Phi_{short-range}$ due to a point charge q_i surrounded by a Gaussian with the net charge $-q_i$:

$$\Phi_{short-range}(r) = \frac{q_i}{r} - \frac{q_i}{r} erf(\sqrt{\alpha}r) = \frac{q_i}{r} erfc(\sqrt{\alpha}r) \tag{6.20}$$

With this result we can finally write the total electrostatic contribution to the potential energy.

$$\begin{aligned} U_{Coul} = &\frac{1}{2V}\sum_{k\neq 0} \frac{4\pi}{k^2} |\rho(\mathbf{k})|^2 e^{(-k^2/4\alpha)} \\ &- (\alpha/\pi)^{\frac{1}{2}} \sum_{i=1}^{N} q_i^2 \\ &+ \frac{1}{2}\sum_{i\neq j} \frac{q_i q_j erfc(\alpha r_{ij})}{r_{ij}} \end{aligned} \tag{6.21}$$

For an efficient way of computing the energies, one combines the Ewald summation with FFT in the so-called Particle mesh Ewald (PME) method. The basic idea remains the same as in Ewald summation. We split the potential in a long and a short-range part, but calculate the charge density field on a discrete lattice (meshing part), which is more efficient via fast fourier transformation. This leads to an algorithm with efficiency $O(N\ log(N))$ in comparison to the direct computation of $O(N^2)$. However, for certain geometries, the Ewald sum is not converging, and furthermore, the method is in principle designed for charge neutral systems. Therefore, different approaches must be considered. One class of algorithms which is converging is the MMM family. The basic difference between the approaches is that one can multiply each summand by a continuous factor $c(\beta, r_{ij}, n_{klm})$ such that the sum is convergent for $\beta > 0$ but $c(0, .., ..) = 1$, instead of defining a summation order as it was done in the Ewald sum. The energy is then defined as the limit of β against 0 of the sum [2].

6.0.2. 2D slab geometry

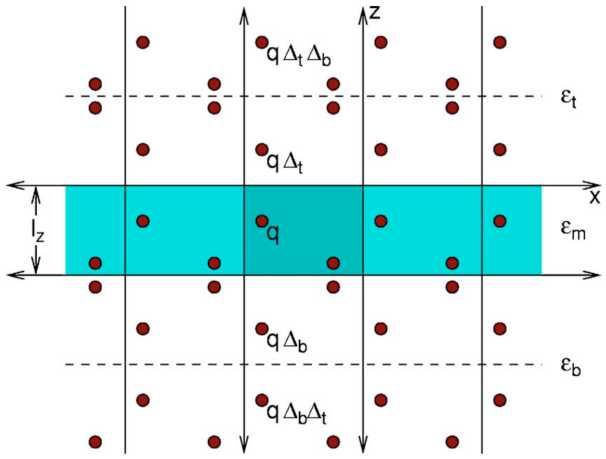

Figure 6.1.: A schematic view of image charges. The dielectric interfaces are characterized by the $\epsilon_t - epsilon_m$ and $\epsilon_m - \epsilon_b$ boundaries. Image charges along the$z$ direction are due to polarization effects. An infinite number of image charges arises along the z direction due to multiple reflections under the two parallel dielectric interfaces. Also shown are the image charges under the periodic boundary conditions along the x axis. The dotted lines are only provided to visualize the positioning of the image charges summation [13]. Tyagi et al, THE JOURNAL OF CHEMICAL PHYSICS 127, 154723 (2007) , Copyright American Institute of Physics (2007)

2D periodic replicated dimensions with a finite third dimension (2D+h) are of special interest regarding the simulation of capacitors, membranes or thin films. There is in principle the possibility to use Ewald summations, but through the finite dimension, there is no straightforward way to use the fast fourier transformation. There is a formalism which explicitly considers one finite length as shown in [7] it is often more

efficient to use a 3D model with an 'electrostatic correction term'. The problem with this approach is that the accuracy is limited by the used implementations of PME and therefore heavily sensitive to the parameter α.
In order to get a better error control and better accuracy, the so-called MMM2D algorithm is a better choice. Starting from two planar, parallel interfaces that enclose a set of charges and there replicated image charges, as shown in figure 6.1, to satisfy the boundary conditions of the electric field. The top and bottom interface of the main cell scale down the image charges by the factor:

$$\Delta_t = \frac{\epsilon_m - \epsilon_t}{\epsilon_m + \epsilon_t} \; and \; \Delta_b = \frac{\epsilon_m - \epsilon_b}{\epsilon_m + \epsilon_b} \tag{6.22}$$

where ϵ_m is the background permittivity in the main cell and ϵ_b,ϵ_t are the corresponding top and bottom media. Considering a charge q, which gets reflected at the top(bottom) interface yields an image of magnitude $q\Delta_t$(resp. $q\Delta_b$). The second reflection yields another image charge $q\Delta_t\Delta_b$ (resp. $q\Delta_b\Delta_t$) in the opposite cell, and so on.
The key idea of MMM2D is to seperate the interaction of two particles into a near and far formula.
Assuming a simulation box of size $L_x \times L_y \times L_z$ that is periodic in x and y dimensions and finite in the z direction. The finite direction is subdivided into k cells which yields to a single cell width of $\lambda = l_z/k$. In general k is chosen in a way that just neighboring cells are interacting through the near formula. To describe MMM2D we assume $\epsilon_m = \epsilon_t = \epsilon_b$, as shown in in figure 6.1. The Coulomb potential of a unit charge is evaluated in Cartesian coordinates with $|z| > 0$, in periodic image charges in the x and y direction, can be written as:

$$\begin{aligned}\Phi(x,y,z) = 4u_x u_y \sum_{p,q>0} \frac{exp^{-2\pi f_{pq}|z|}}{f_{pq}} cos(w_p x) cos(w_q y) \\ + 2u_x u_y \left(\sum_{p>0} \frac{exp^{-2\pi f_p|z|}}{f_{pq}} cos(w_p x) + \sum_{q>0} + \frac{exp^{-2\pi f_q|z|}}{f_{pq}} cos(w_q y) \right) - 2\pi u_x u_y |z|\end{aligned} \tag{6.23}$$

where $(x,y,z) = (x_{ij}, y_{ij}, z_{ij})$, p and q are integer, $u_x = 1/l_x$, $u_y = 1/l_y$, $f_{pq} = \sqrt{(u_x p)^2 + (u_y q)^2}$ with $f_p = pu_x$, $f_q = qu_y$ and $w_p = 2\pi u_x p$, $w_q = 2\pi u_y q$.
The far formula convergences for $|z| \to \infty$ and divergences for $|z| \to 0$. To handle this problem we introduces the near formula in the case of $0 < |z| < 2\lambda$, i.e. neighboring

cells.

$$\Phi(x,y,z) = 4u_x \sum_{l,p>0} [K_0(\omega_p \rho_l) + K_0(\omega_p \rho_{-l})] cos(\omega_p x) \tag{6.24}$$

$$- 2u_x \sum_{n\geq 1} \frac{b_{2n}}{2n(2n)!} Re[(2\pi u_y (z+iy))^{2n}]$$

$$- u_x \sum_{n\geq 1} \binom{-1/2}{n} \frac{\Psi^{(2n)}(N_\Psi - u_x x) + \Psi^{(2n)}(N_\Psi + u_x x)}{(2n)!} (u_x \rho_0)^{2n} \tag{6.25}$$

$$- 2u_x log(4\pi \frac{u_y}{u_x}) + \sum_{k=1}^{N_\Psi} \left(\frac{1}{r_k} + \frac{1}{r_{-k}} +' \frac{1}{r_0} \right)$$

where $\rho_l = \sqrt{(y+ll_y)^2 + z^2}, r_k = \sqrt{(x+kl_x)^2 + y^2 + z^2}$, K_0 denotes the Bessel function of second kind, b_n denotes the Bernoulli numbers and $\Psi_{(n)}$ stands for the Hankel function of order n. N_Ψ is a tuning parameter and commonly chosen to be 2. The interaction between a charge and its own image charges along x and y, is calculated by the near formula, whereas the last term has to be left out by the prime. The total electrostatic energy of a set of N charges can be obtained by pairwise addition and using the near and far formula.
The pairwise calculation using the far formula of the energy results in a N^2 scaling. Fortunately product decomposition is a property of the far formula, which improves the computation of the interaction between two sets of charges to linear scaling. Computing eight factors $\Xi^{\pm s/c, s/c}(p,q)$ for a group of charges and frequency components (p,q):

$$\Xi^{\pm s/c, s/c}(p,q) = \sum_{q_i \in L} q_i exp(\pm 2\pi f_{pq} z_i) sin/cos(w_p x_i) \ \times \sin / \cos(w_q y_i) \tag{6.26}$$

In order to take dielectric layers into account we are use the method of image charges (ICMMM2D). We assume that two interfaces are located at $z = 0$ (bottom) , $z = l_z$ (top) and surround N charges particles in central dielectric layer. The charges are labeled q_i form 1 to N. This leads to image charges along the z direction and in addition repeated image charges of image charges due to the two planar dielectric layers. For each of the lower and upper layers, the separation of image charges into two sequences. Assuming a charge q_i at position z_i results into the two sequences regarding the lower dielectric domain:

charge $q_i\Delta_b$, $q_i\Delta\Delta_b$, $q_i\Delta^2\Delta_b$, ...
position $-z_i$, $-(2l_z + z_i)$, $-(4l_z + z_i)$, ...
and
charge $q_i\Delta$, $q_i\Delta^2$, $q_i\Delta^3$, ...
position $-(2l_z - z_i)$, $-(4l_z - z_i)$, $-(6l_z - z_i)$, ...,
where $\Delta = \Delta_b\Delta_t$. Similar for the upper layer.
Now we consider how to incorporate all the interactions of the charges with the image

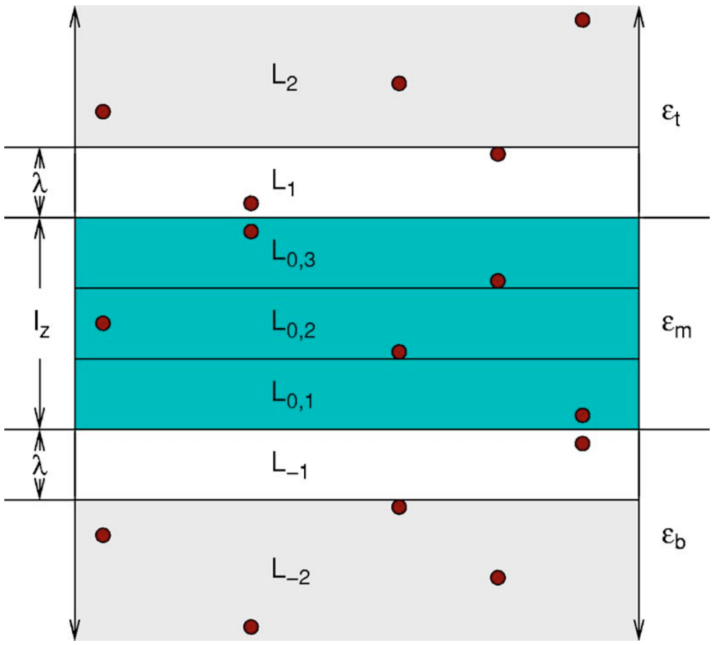

Figure 6.2.: A schematic view of the simulation cell for $k = 3$. The original cell is divided into three layers. The top dielectric ϵ_t region is divided into two cells, L_{+1} and L_{+2}. Similarly, the bottom dielectric region ϵ_b is divided into two regions L_{-1} and L_{-2}. Note that L_{-2} and L_{+2} extend to $-\infty$ and ∞ , respectively. Tyagi et al, THE JOURNAL OF CHEMICAL PHYSICS 127, 154723 (2007) , Copyright American Institute of Physics (2007) [13].

charges in an efficient way. We subdivide the original charges into layers of height λ to sets $L_{0,i}i = (1, 2, ...k)$ and the upper and lower layers into layers $L_-/L+ = L_{-1} + L_{-2}/L_{+1} + L_{+2}$,as illustrated in figure 6.2. The thickness of the layer next to the center cell is λ, whereas the second layer extends from λ to infinity. By summing over all charges in the lower layer L_-, we find geometric sums and define :

$$L_{p,q}(z) = \sum_{m=0}^{\infty} \Delta^m exp[-2\pi f_{pq}(z + 2ml_z)] = \frac{e^{(-2\pi f_{pq} z)}}{1 - \Delta exp(-4\pi l_z f_{pq})} \tag{6.27}$$

Note that the layers next to the boundary, i.e. $L_{0,1}$ and L_{-1} require the use of the near formula, but however the interaction of $L_{0,1}$ with L_{-2} requires the far formula. Furthermore for all interactions of $L_{0,i}$ $(i = 2, 3, 4, .., k)$ with L_- the calculation via far formula is needed as well as for L_+ [13].

7. Results

7.1. Single charge in 2D+h

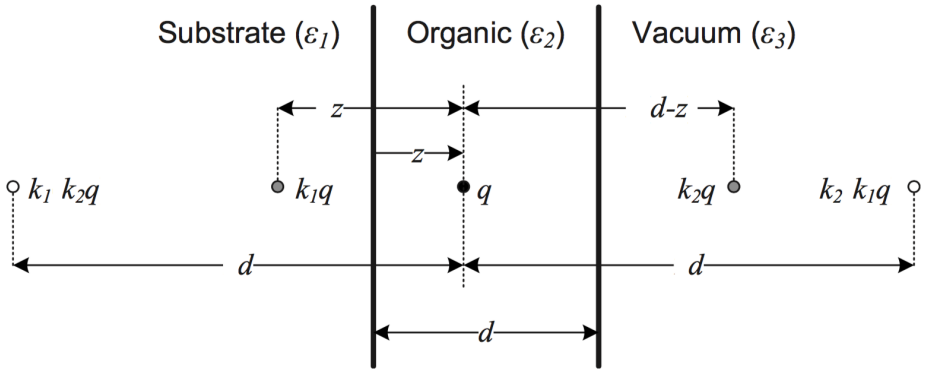

Figure 7.1.: A Dielectric continuum model of an organic overlayer on a substrate with point charge $q = e$ in the organic layer. 1, 2, and 3 are the permittivities of each layer and $k1$ and $k2$ are the reflection coefficients at the dielectric boundaries. The image charges shown are from the $n = 0$ term of 7.4.Helander et all, Physical Review B 81,153308 (2010) , Copyright The American Physical Society (2010) [5].

In this chapter we compare the direct calculation, the ICMMM2D technique as well as analytic solution. We like to evaluate single and two particle Green's functions which are needed to efficiently construct energy difference required to run KMC code. First of all, we like to study the behaviour of the ICMMM2D algorithm for different sizes of periodic boxes along the x- and y-directions. We expect that the potential energy will get lower for larger system sizes. Figure 7.2 shows a gain of potential energy by expanding the system in the periodic directions. The gain of energy means that image charges along the z-direction have a greater influence in comparison to the replicated charges in x and y in an extensive system even through the reduction of the image charged by the refection coefficients. We use to compare the ICMMM2D with the direct sum of the Coulomb interaction based on the electrostatic potential of a collection of N charges:

$$E_{total} = \frac{1}{4\pi\epsilon_0} \sum_{i=1}^{\infty} Q_i \phi_i, \text{ where } \phi_i = \frac{1}{4\pi\epsilon_0} \sum_{j=1(i\neq j)}^{\infty} \frac{Q_j}{r_{ij}}, \tag{7.1}$$

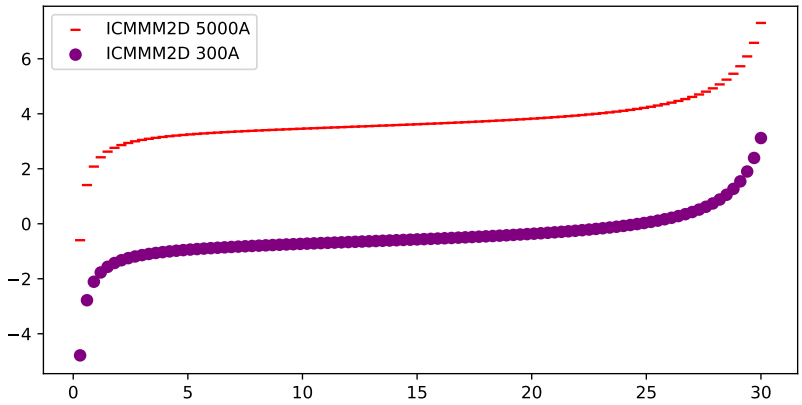

Figure 7.2.: Comparison of ICMMM2D for different system sizes concerning the x- and y- direction

$E_{total} = \frac{1}{4\pi\epsilon_0}\sum_{i=1}^{\infty} Q_i\psi_i$, $with\ \psi_i = \frac{1}{4\pi\epsilon_0}\sum_{j=1(i\neq j)}^{\infty}\frac{Q_j}{r_{ij}}$where $r_{ij} = r_i - r_j$.

Despite we are in a 2d+h geometrie, we will use an Ansatz which is used in 3D PBC.

$$E = \frac{1}{4\pi\epsilon}\frac{1}{2}\sum_{i=1}^{N}\sum_{i=1}^{N}\sum_{\mathbf{n}}^{\dagger}\frac{q_i q_j}{|\mathbf{r}_i j + \mathbf{nL}|}, \tag{7.2}$$

where L is a vector that consists the box expansion and $\epsilon = \epsilon_{vacuum}\epsilon_{subtract}$. The sum over $\mathbf{n}$ is running over all lattice point2 $\mathbf{n} = (n_x L_x, n_y L_y, n_z L_z)$ with integers n_x, n_y, n_z. The † symbolizes that we omit $i = y$ for $\mathbf{n} = (0, 0, 0)$ in the main cell to avoid double counting. The derived sum conditionally converges for a defined way of summing up the independent terms (spheric, cubic, cylindric, etc.). We are going to use a cubic system to perform the calculations. Even in a cubic system, one is just able to calculate the direct sum for a few replicas and heavily relies on a cut-off for n because the algorithm scales with $O(n_{cut}^6 N_{particle}^2)$. The performed calculations show that it was sufficient to choose $n = 11$. In order to come closer to the slab geometry we can choose different replica box numbers along the finite z and infinit x and y direction. And take into account that the charge in z direction is changing through the respective reflection coefficients. In principle we split the sum in 4 terms which are corresponding charge sequences used in the ICMMM2D. charge $q_i\Delta_b$, $q_i\Delta\Delta_b$, $q_i\Delta^2\Delta_b$, ...

position $-z_i$, $-(2l_z + z_i)$, $-(4l_z + z_i)$, ...

and

charge $q_i\Delta$, $q_i\Delta^2$, $q_i\Delta^3$, ...

position $-(2l_z - z_i)$, $-(4l_z - z_i)$, $-(6l_z - z_i)$, ..., To simulate a particle in between metal, we need to take the images charges at the boundaries into account. To perform a similar calculation in espresso, we need to set the parameters. ICMMM2D requires as parameters the charge position, the charge itself, the reflection coefficients k_1, k_2,

and a prefactor $C = \frac{1}{4\pi\epsilon_{vaccum}\epsilon_2}$.

$$k_1 = \frac{\epsilon_2 - \epsilon_1}{\epsilon_2 + \epsilon_1} \; and \; ak_2 = \frac{\epsilon_2 - \epsilon_3}{\epsilon_2 + \epsilon_3} \tag{7.3}$$

where ϵ_1 and ϵ_3 are the permittivities of the layer along the z-direction which surround the subtract layer with permitivitty ϵ_2. In VOTCA we are able to simulate a few hundred nanometers of a semiconductor. Therefore an appropriate choice of the layer thickness along the z-direction is $300\mathring{A}$. In theory, the potential energies of the ICMMM2D calculations will converge against the direct sum value for large x and y expansions, due to the small interactions of the replicas in this directions. Because ICMMM2D is optimized for smaller applications, the calculations will need longer for each magnitude enlargement. Hence we choose $10000\mathring{A}$ as the length in $x-$ and $y-$direction and $k_1 = 0.5$ and $k_2 = -1$. In figure 7.3 we see that even when we just use the direct sum without taking the reflection coefficiants into account the results fit in-between the slap but the potential is as expected stronger at the boundaries.

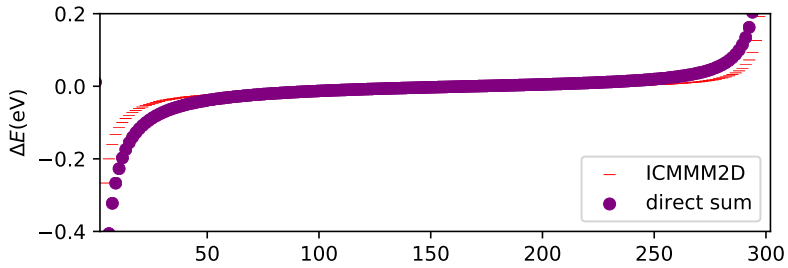

Figure 7.3.: Comparison of direct sum and ICMMM2D algorithm for a test particle moving along the z direction

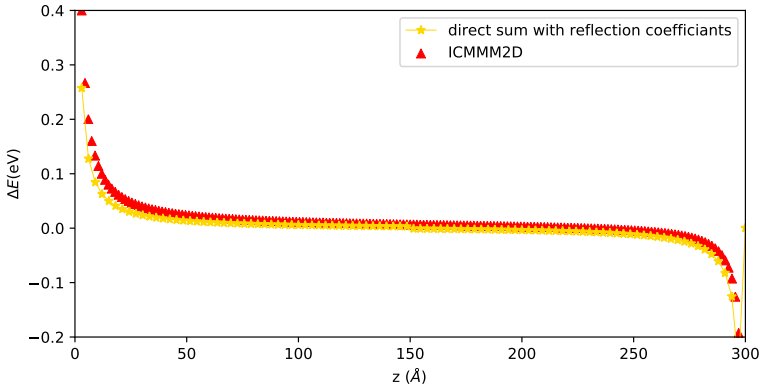

Figure 7.4.: Comparison of direct sum that includes reflection coefficants and ICMMM2D algorithm for a test particle moving along the z direction

By taking in figure 7.4 the reflections coefficiants into account we see that the screening of the ICMMM2D and the direct sum at the boundaries is better. A different approach is to construct a classical dielectric model consisting of three dielectric layers, with permittivities of ϵ_1, ϵ_2 and ϵ_3, in contact with each other to test the screening of the ICMMM2D method. The system is composed of a subtract slab ($z < 0$), an organic layer of thickness $d(0 < z < d)$ and the vacuum film ($z > d$). The typical approach to deal with dielectric boundaries it as mentioned before the method of image charges as shown in figure 7.1. Therefore we assume in a z-direction a periodic repetition of duplicates, based on the original box. The Each boundary lead to reflection coefficients that are defined as Based on the position and charges presented in the chapter '2D slab geometrics' it is simple to calculate a 1-dimensional solution for the Coulomb interaction of a particle with its image

$$\Delta E = \frac{e^2}{16\pi\epsilon_0\epsilon_2}\sum_{n=0}^{\infty}(k_1k_2)^2\left(\frac{k_1}{z+nd}+\frac{k_2}{(n+1)d-z}+\frac{2k_1k_2}{(n+1)d}\right) \tag{7.4}$$

charges.

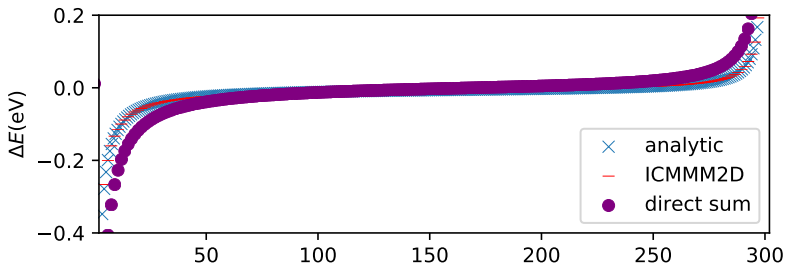

Figure 7.5.: Comparison of analytical and ICMMM2D algorithm for a test particle moving along the z direction

The plot 7.5 shows that the analytic and the ICMMM2D approach are much better in treating with the different dielectric interfaces compared to the direct sum. The direct sum is taken into account the enlargement of the distance between the particles, but the reduction of the charge due to reflection coefficients are neglected. However we are able to improve the result of the algorithm. Therefore we have to remember that we are using the concept of image charges to simulate boundaries and exploiting the systems periodicity. We are not able to place two image charges in the cells left and right of the main cell cause higher order terms are canceling and we get an infinite term. This can be handled by changing the image charge position form the left cell to the right in the case that the test particle crosses the middle of the cell. The plot A.1 in the appendix uses $k_1 = k_2 = -1$ and one observes a much better fitting of the direct sum. At this point should be mentioned that the direct sum and the analytical approach avoids the energy artefacts due to the artificial divergence of classical electrostatics near the vacuum interface of the dielectric continuum model [5]. This effect affects the smaller system more than a larger system. Additionally, the

direct sums and the ICMMM2D algorithm are converging into interactions which are observed for just two image charges in large classical systems.
So far we noted that a charge carrier is behaving as expected in between the applied boundaries, but we are interested in the way a carrier interact with further carries. The interaction will be important because we are interested in the calculation the interaction matrix even for the analytic solution. Therefore the next step will be to test the how the algorithm handles more particles and calculate a pair interaction matrix. So far we noted that a charge carrier is behaving as expected in between the applied boundaries, but we are interested in the way a carrier interact with further carries. The interaction will be important because we are interested in the calculation the interaction matrix even for the analytic solution. Therefore the next step will be to test the how the algorithm handles more then just one particle to see if the implementation does not just treat the boundaries of the system correctly. Therefore the injection of a second particle with charge e at fix position is the next test case, whereas the calculation of the interaction remains the same as before. The comparison of 7.7 a) and b) shows that we get a sufficient approximation of a semiconductor, due to applying the direct sum on the electrostatic properties but for further comparison, we need to rely on the analytic approach. But on the other hand, the direct sum leads to the same results as the other applied methods if we choose $k_1 = k-2$,i.e. we considering a symmetrical systems. This means that we have found a tool to compare the calculation of the ICMMM2D interaction matrix at least for same reflection coefficients. But what is a good approach to deal with the pair interaction in semiconductor? The idea is to expand the analytic approach which yields matching result for the semiconductor case into x- and y-direction.

7.2. Pair interaction matrix on the example of CBP

To evaluate the total electrostatics in the Thole model, we are interested in expanding the pair interacting matrix G_{ij} regarding multipoles. The pair interacting matrix is nothing as a matrix which consists of all interactions of carrier vector i and j and gives the total energy of the system by summing over all charges:

$$E_{total} = \frac{1}{2} \sum_{ij} q_i^T G_{ij} q_j. \tag{7.5}$$

As test case we choose a system of 500 CBP molecules with 5000 sites which can interact with each other as shown in 7.9
Due to the constructing of G_{ij}, it is evident that the matrix needs to be symmetric. From a computational point of view, it is enough to determine the upper triangle or lower half triangle part. To test if the ICMMM2D algorithm preserves the right predictions, it will be enough to check if the matrix is symmetric because we examine the static behaviour before. Due to slow performance 3d analytic approach and the direct sum we need to reduce the system size. We do not need to treat the diagonal elements of G_{ij} in this thesis because they need a special treating due to the self-action

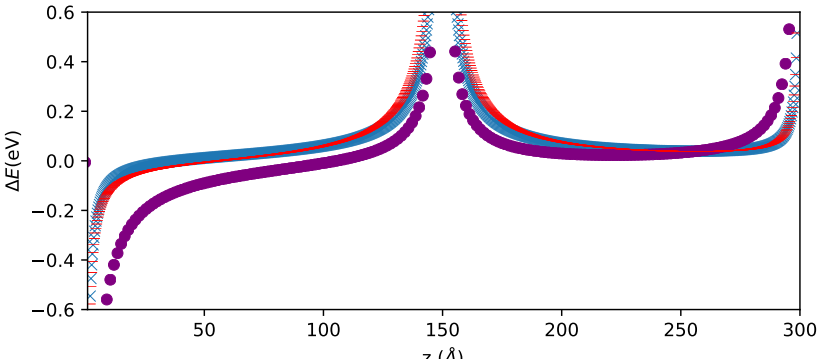

Figure 7.6.: semiconductor boundaries $k_1 = 0.5, k_2 = -1$

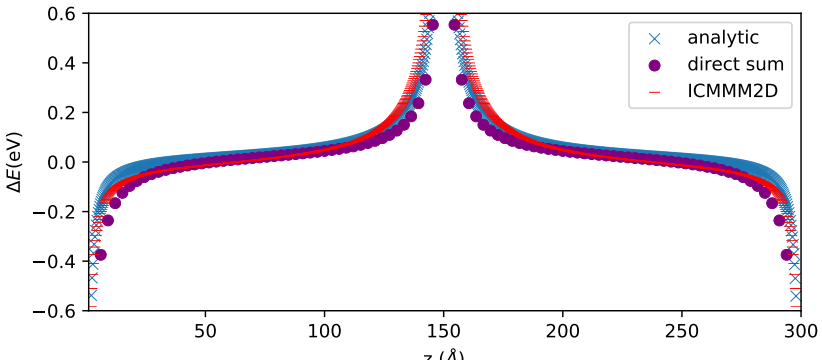

Figure 7.7.: metal boundaries $k_1 = k_2 = -1$

Figure 7.8.: Comparison of analytical, direct sum and ICMMM2D algorithm for a test particle moving along the z direction with a fix charge carrier in the center box

nature. We can use $\vec{q_i}$ and $\vec{q_j}$ which consists of 4999 components which are 0 and one which is 1.Even so, in order the present them we going to use each 1000 element so that we will see a $5x5$ matrix. The ICMMM2D matrix,

$$M_{ICMMM2D} = \begin{pmatrix} g_{1,1} & -0.04716 & -0.04805 & -0.04950 & 0.00552 \\ -0.04717 & g_{1000,1000} & -0.1156 & -0.09630 & -0.07362 \\ -0.04806 & -0.15569 & g_{2000,200} & -0.08597 & -0.06694 \\ -0.04951 & -0.09630 & -0.08597 & g_{4000,4000} & -0.03476 \\ 0.00552 & -0.07362 & -0.06694 & -0.03476 & g_{5000,5000} \end{pmatrix}$$

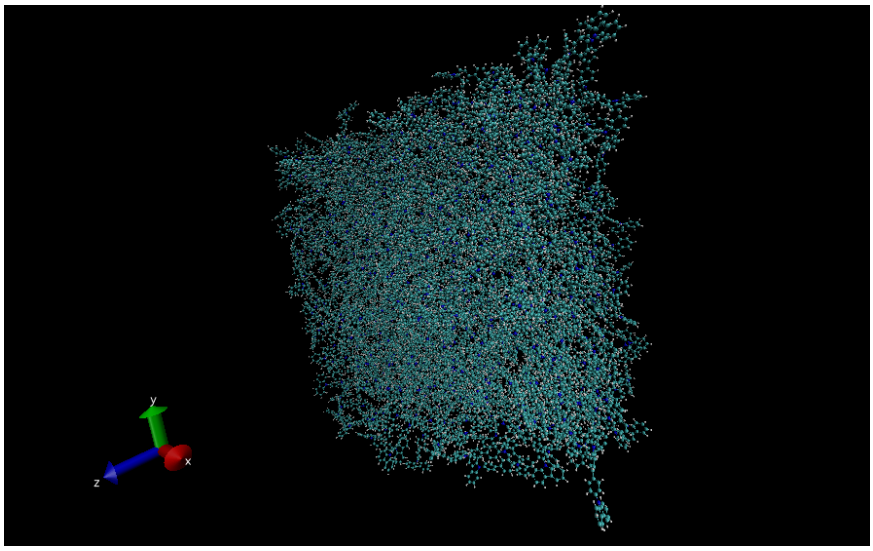

Figure 7.9.: System of 500 CBP molecules

and the direct sum matrix

$$M_{directsum} = \begin{pmatrix} g_{1,1} & -0.06171574 & -0.0689306 & -0.1488697 & -0.3166535 \\ -0.1520251 & g_{1000,1000} & -0.118146 & -0.1722671 & -0.2951772 \\ -0.1516867 & -0.1264734 & g_{2000,200} & -0.1439937 & -0.2731144 \\ -0.1516867 & -0.1264734 & -0.1264734 & g_{4000,4000} & -0.2731144 \\ -0.0937269 & -0.08631007 & -0.1065622 & -0.1396134 & g_{5000,5000} \\ . & & & & \end{pmatrix}$$

We observe for the ICMMM2D, and the direct sum results are in the same order of magnitude but that the direct sum matrix is not symmetric. This means that we get different result taking for exchanging the vectors q_i and q_j. Therefore we are not able to apply the method to adding carriers with the opposite sign to the system anymore to simulate dielectric contrast anymore. Unfortunately, the expansion of the analytic approach has the same problem that the solution is not equal under exchanging carriers. Dos Santos et al. provide a different method with the calculate the pair interactions in 2d+h geometries. [1] Unfortunately, they just provide a solution for the energy if we assume the same dielectrica at the boundaries. To get a more general solution, we need to a little effort into it. We will start from the electrostatic potential at $\mathbf{r} = (x, y, z)$ that satisfies the Poisson equation:

$$\nabla^2 G(r, r_i) = \frac{4\pi q_i}{\epsilon_2} \sum_{nx,ny=-\infty}^{\infty} = \delta(\mathbf{r} - \mathbf{r}_i + n_x L_x \mathbf{x} + n_y L_y \mathbf{y}). \tag{7.6}$$

The periodic delta function can be Fourier transformed to:

$$\sum_{nx,ny=-\infty}^{\infty} \delta(x-x_i+m_xL_x)\delta(y-y_i+m_yL_y) = \frac{1}{L_yL_x} \sum_{nx,ny=-\infty}^{\infty} e^{i[\frac{2\pi m_x}{L_x}(x-x_i)+\frac{2\pi m_y}{L_y}(y-y_i)]}, \tag{7.7}$$

where **n** are the Fourier modes. The Green function now takes the form:

$$G(\mathbf{r},\mathbf{r}_j) = \frac{1}{L_xL_y} \sum_{nx,ny=-\infty}^{\infty} g_{\mathbf{n}}(z_i,z) \exp^{i[\frac{2\pi m_x}{L_x}(x-x_i)+\frac{2\pi m_y}{L_y}(y-y_i)]}. \tag{7.8}$$

By intersecting eq. 7.8 into 7.6 one find:

$$\frac{\partial^2 g_{\mathbf{m}}}{\partial z^2} - k^2 g_{\mathbf{m}}(z_i,z) = \frac{-4\pi q_i}{\epsilon_{subtract}}\delta(z-z_i), \tag{7.9}$$

where $k = 2\pi\sqrt{m_x^2/L_x}$. The general solution has the form $Ae^{-kz} + Be^{kz}$. By using that the potential will be vanishing as $z- > \pm\infty$ and need to be dacay exponentially in the outsight the box. The symmetry of the green function in combination with the applied boundaries are defining:

$$g_{\mathbf{n}}(z_i,z) = \frac{2\pi q_i}{\epsilon_{vacuum}}[e^{-k|z-z_i|} + \Delta e^{-k(z+z_i)} + \Delta e^{-2kL_z}e^{k(z+z_i)} + \Delta^2 e^{(-2kL)}e^{k|z-z_i|}], \tag{7.10}$$

where Δ is the usual reflection .
With this method we are able to calculate an symmertic matrix, but we observe the same problem as for the fast fourier transformation. There is a high number of fourier modes that needed to be calculated due to the small system size and this methode needs further proceeding.

$$M_{Green} = \begin{pmatrix} g_{1,1} & 0.02345 & 0.02345 & 0.02345 & 0.02345 \\ 0.02345 & g_{1000,1000} & 0.00058 & 0.02345 & -0.0002 \\ 0.02345 & 0.00058 & g_{2000,200} & 0.02346 & 0.023460 \\ 3.75315 & 0.02345 & 0.02346 & g_{4000,4000} & -0.02345 \\ 0.02345 & -0.0002 & 0.02346 & 0.02345 & g_{5000,5000} \\ . & & & & \end{pmatrix}$$

8. Conclusion and Outlook

I showed that one needs to rely on scholastic models to calculate the charge carrier mobility and the charge carrier density probability. To solve this problem regarding time evolution the stochastic model of choice is the master equation which is frequently addressed by KMC methods. But in order to do so the calculation of hopping rates in each time step is essential. These calculations are computational demanding due to the long-range character of the Coulomb interaction.
In this thesis, I showed that the ICMMM2D algorithm is efficient choice to calculate the Coulomb interaction in slab geometries. The treatment of dielectric contrast tested by comparing the results with the analytic solution, whereas a comparison with the direct sum showed an appropriate treatment of multiple carriers. The ICMMM2D algorithm leads to acceptable result regarding calculating pair interactions with a significant decrease in computational time. The matrix consisting of all pair interaction can be easily expanded into multipoles as it is shown in chapter 1. This expansion can be used to build a Thole mode which is needed to perform the rate calculation in the KMC algorithm in VOTCA. In the end, we could perform more efficient simulations in 2d+h geometries due to the efficient performance of the ICMMM2D regarding error estimation and accuracy.

A. Appendix

A.1. Figures

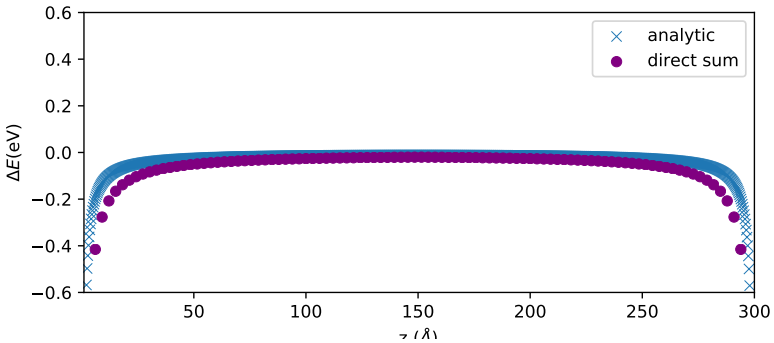

Figure A.1.: Solution for $k_2 = k_1 = -1$

List of Figures

@articleslab, Author = In-Chul Yeh, Max L. Berkowitz, Date-Added = 2018-02-15 10:00:46 +0000, Date-Modified =2018-02-15 10:01:35 +0000, Journal = The Journal of Chemical Physics, Number = 3155, Title = Ewald summation for systems with slab geometry, Volume = 111, Year = 1999

Bibliography

[1] Matheus Girotto Alexandre P. dos Santos and Yan Levin.
Simulations of coulomb systems confined by polarizable surfaces using periodic green functions.
The Journal of Chemical Physics 147,, 2017.

[2] Axel Arnold.
Computer simulations of charged systems in partially periodic geometries.
PhD thesis, Johannes Gutenberg–Universität, 2004.

[3] Appl. C. W. Tang.
Appl. Phys. Lett., 1986.

[4] J. Cottaar and P. A. Bobbert.
Calculating charge-carrier mobilities in disordered semiconducting polymers: Mean field and beyond.
Physical Review B, 74(11), Sep 2006.

[5] M. G. Helander, M. T. Greiner, Z. B. Wang, and Z. H. Lu.
Effect of electrostatic screening on apparent shifts in photoemission spectra near metal/organic interfaces.
Physical Review B, 81(15), Apr 2010.

[6] Ronald A. Howard.
Dynamic Probabilistic Systems, volume 1: Markov Chains.
Dover Books on Mathematics, 1971.

[7] Max L. Berkowitz In-Chul Yeh.
Ewald summation for systems with slab geometry.
The Journal of Chemical Physics, 111(3155), 1999.

[8] John W. Tukey James W. Cooley.
An algorithm for the machine calculation of complex fourier series.
Math. Comput., 19(19):297–30, 1965.

[9] A.P.J. Jansen.
An Introduction to Kinetic Monte Carlo Simulations of Surface Reactions.
Springer, 2012.

[10] Pascal Kordt.
Charge Dynamics in Organic Semiconductors.
PhD thesis, Johannes Gutenberg Universtiät Mainz, 2015.

[11] Pascal Kordt, Jeroen J. M. van der Holst, Mustapha Al Helwi, Wolfgang Kowalsky, Falk May, Alexander Badinski, Christian Lennartz, and Denis Andrienko.

Modeling of organic light emitting diodes: From molecular to device properties. *Advanced Functional Materials*, 25(13):1955–1971, Jan 2015.

[12] Anthony Stone.
The Theory of Intermolecular Forces.
Oxford University Press, 2016.

[13] Sandeep Tyagi, Axel Arnold, and Christian Holm.
Icmmm2d: An accurate method to include planar dielectric interfaces via image charge summation.
The Journal of Chemical Physics, 127(15):154723, Oct 2007.

[14] Piet Th. van Duijnen* and Marcel Swart.
The Journal of Chemical Physics, 1998.

B. Acknowledgment

Dennis Andrienko and Leanne Paterson for the supervision and help in editing the thesis.